Quantum Electronics 24 (7) 632–635 (1994)

PACS numbers: 42.65.An; 42.62.Hk; 42.65.Ky; 72.40.+w

Transient gratings of a quadratic nonlinear susceptibility due to the coherent photogalvanic effect in semiconductor-microcrystallite-doped glasses

E M Dianov, P G Kazanskiĭ, D S Starodubov

Abstract. A fast (transient) component of the photoinduced quadratic (second-order) susceptibility was observed in a glass doped with CdS_xSe_{1-x} semiconductor microcrystallites. The experimental results, obtained by a new method involving counterpropagating write and read pulses, confirmed the photogalvanic nature of the effect.

1. Introduction

Glasses do not have a quadratic (second-order) susceptibility $\chi^{(2)}$ because of their centrosymmetric structure. Therefore, the majority of the nonlinear effects observed in fibre-optic waveguides are associated with a higher-order (cubic) nonlinear susceptibility $\chi^{(3)}$. An unusually efficient (with an efficiency up to 5%) process of second-harmonic generation (SHG) was first observed in a germanosilicate glass fibre in 1986 by Osterberg and Margulis [1] after the fibre was exposed for 12 h to high-power radiation from a Q-switched and mode-locked YAG:Nd laser. The second-harmonic power obtained in this way was sufficient to pump a commercial dye laser [1].

2. Models of the effect

Two groups of models have been proposed to account for the photoinduced SHG in glasses. According to some models, the quadratic nonlinearity is due to the orientation of dipoles, whereas according to other models it is associated with macroscopic separation of charges because of the coherent photogalvanic effect or because of diffusion. The fate of the macroscopic model has been settled finally by experimental investigations of the spatial distribution of the quadratic nonlinearity of bulk glass samples. Different models predict fundamentally different distributions. It has been found that macroscopic separation of charges occurs in single-phase glasses because of the coherent photogalvanic effect [2] and the movement of space-charge regions has been observed [3]. These experiments fully support the models based on the coherent photogalvanic effect.

E M Dianov, D S Starodubov Fibre Optics Research Centre at the Institute of General Physics, Russian Academy of Sciences, Moscow
P G Kazanskiĭ Optoelectronics Research Centre, Southampton University, Southampton, England

Received 11 March 1994
Kvantovaya Elektronika 21 (7) 685–688 (1994)
Translated by A Tybulewicz

The coherent photogalvanic (photovoltaic) effect represents the appearance of a direct current in a centrosymmetric or noncentrosymmetric medium when it is homogeneously illuminated with fundamental-frequency radiation and with the second harmonic [4–7]. This effect is similar to the familiar bulk photogalvanic effect observed in noncentrosymmetric media. The coherent photogalvanic effect may be the result of interband, impurity–band, or intraband transitions. The following phenomenological expression describes the density of the photogalvanic current:

$$\begin{aligned} j_{\rm ph} = {} & \beta_b(E_\omega E_\omega^* + E_{2\omega}E_{2\omega}^*) + \beta E_\omega E_\omega E_{2\omega}^* \exp(i\Delta kz) \\ & + \beta_1 E_\omega E_\omega E_\omega E_\omega^* E_{2\omega}^* \exp(i\Delta kz) \\ & + \beta_2 E_\omega E_\omega E_{2\omega} E_{2\omega}^* E_{2\omega}^* \exp(i\Delta kz) \\ & + \beta_3 E_\omega E_\omega E_\omega E_\omega E_\omega^* E_\omega^* E_{2\omega}^* \exp(i\Delta kz) + \text{c.c.}\,, \end{aligned} \tag{1}$$

where the first component is the photocurrent associated with the bulk photogalvanic effect (it is absent in the case of glasses because they are centrosymmetric); the second component is the lowest-order coherent photocurrent generated by interference between processes involving three coherent photons, i.e. interference between two-photon absorption of the pump (fundamental-frequency) radiation and one-photon absorption of the second harmonic [4–8]; the third and higher components are associated with higher-order coherent processes [9]; β_b, β, β_1, β_2, and β_3 are the corresponding photogalvanic constants; E_ω and $E_{2\omega}$ are the amplitudes of the electric fields of the pump and second-harmonic waves; $\Delta k = 2k_\omega - k_{2\omega}$. Under steady-state conditions the photogalvanic effect creates an electrostatic field $\mathscr{E}_{\rm dc}$ in a medium as a result of compensation of the photogalvanic current by the drift current: $\mathscr{E}_{\rm dc} = -j_{\rm ph}/\sigma$, where σ is the photoconductivity. This field induces the quadratic susceptibility $\chi^{(2)}$ via the cubic susceptibility: $\chi^{(2)} = 3\chi^{(3)}\mathscr{E}_{\rm dc}$.

In contrast to single-phase systems, in which macroscopic separation of charges is observed, there is no macroscopic charge transfer [2] in a glass doped with semiconductor microcrystallites (GDSM) in which quasi-phase-matched photoinduced SHG can take place [11]. This result is logical if we assume that the formation of a grating involves processes occuring inside the semiconductor microcrystallites [11].

The process of photoinduced SHG in a GDSM can be explained [2] by the separation of charges because of the coherent photogalvanic effect inside the microcrystallites. Studies of the temperature dependences demonstrate a considerable difference between the microscopic mechanisms of the photoinduced SHG in a GDSM and in a lead glass.

In the former case the density of the photogalvanic current increases when the density of thermalised carriers increases, and it is concluded that the photogalvanic effect is due to these carriers [10, 4].

However, a different mechanism may account for the photoinduced SHG in a GDSM. Estimates indicate that a strong electrostatic field due to the polarisation P_{dc} at zero frequency may appear inside the microcrystallites: $\mathscr{E}_{dc} = P_{dc}/\varepsilon_0\chi^{(1)}$, where ε_0 is the permittivity of vacuum and $\chi^{(1)}$ is the linear susceptibility of the microcrystallite medium. A static polarisation appears because of a third-order nonlinear process, similar to the optical rectification effect [11–13]:

$$P_{dc} = \tfrac{3}{8}\varepsilon_0\chi^{(3)}(0 = \omega + \omega - 2\omega)|E_\omega E_\omega E^*_{2\omega}|\cos(\Delta kz) \ . \quad (2)$$

The estimates obtained [11] indicate that such electrostatic fields (of intensity right up to 10^8 V m^{-1}) are quite sufficient to account for the experimentally observed nonlinearities. The available experimental data are insufficient to separate the contributions of the optical rectification and photogalvanic effects to the quadratic nonlinearity. We shall propose an experimental method involving a 'readout' of the photoinduced quadratic nonlinearity at the moment of action of a 'write' pulse. This method makes it possible to separate the photogalvanic contribution from that associated with the optical rectification effect [14].

3. Basic idea of the experiments

A considerable difference between the photogalvanic and optical rectification mechanisms appears only during the action of a write pulse. If the optical rectification effect makes the dominant contribution, the electrostatic field is maximal at the initial moments and then, as a grating of the quadratic nonlinearity forms, the drift current of the charges compensates for (reduces) the initial field. In the case of the coherent photogalvanic effect the electrostatic field is absent at the initial moments of the formation of a grating and then this field rises continuously as the grating is formed. Therefore, the field-induced quadratic susceptibility measured during the action of a write pulse should decrease in the optical rectification effect and rise continuously if the photogalvanic mechanism applies.

4. Investigated sample

A sample of ZhS18 commercial glass was investigated. It was known to have 50% transmission at the wavelength of 505 nm when the thickness was 3 mm. The preparation of a GDSM consisted of two stages: founding of the glass and thermal formation of microcrystallites. The first stage produced an initial uncoloured glass containing cadmium, sulfur, and selenium impurities. In the second stage this glass was heated to 500 °C – 700 °C, which produced semiconductor microcrystallites that imparted colour to the glass. As the microcrystallites grew, the optical transmission edge shifted towards the red wavelengths. Typical dimensions and concentrations of the microcrystallites depend on the initial composition of the glass, and on the temperature and duration of the second stage. In a specially prepared GDSM the microcrystallite size can be a few nanometres, comparable with the Bohr radius of an exciton. This should give rise to size effects, and such a glass is said to contain quantum dots. In the case of Russian commercial GDSMs a typical microcrystallite size is 15 – 30 nm and the concentration of the crystalline phase is a fraction of 1%. Usually a series of glasses of the same type, for example ZhS, are prepared from a material with the same initial composition but subjected to heat treatments of different durations. The glass designated ZhS18 is the last member of this series and contains the largest microcrystallites, so that the size effects can be ignored.

5. Experiments

We used the apparatus shown schematically in Fig. 1. A Q-switched and mode-locked YAG : Nd laser was employed. The repetition frequency of packets consisting of 30 pulses of 600 ps duration was 6.3 kHz. The second harmonic was generated in a KTP crystal. The polarisations of the write and read radiations were the same and were set by two Glan prisms. The read arm contained a delay line which made it possible to superimpose the write and read pulses in a sample. The average power of the read beam was 1.2 W, the power of the pump (fundamental-frequency) write radiation was 0.3 W, and the power of the second-harmonic write radiation was 0.5 mW.

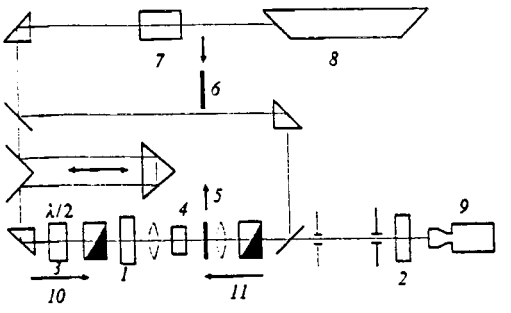

Figure 1. Schematic diagram of the apparatus used in an investigation of the photoinduced second-harmonic generation by a method with counterpropagating write and read pulses: (*1*, *2*) optical filters separating infrared radiation and the second-harmonic, respectively; (*3*) $\lambda/2$ (1.064 nm) plate used to alter the power of the read pulse; (*4*) sample of ZhS18 glass doped with CdS_xSe_{1-x} microcrystallites. Opening of the first shutter (*5*) corresponded to the beginning of the recording and the closing of the second shutter (*6*) to the completion of the recording and observation of the relaxation of the photoinduced second-harmonic signal; (*7*) KTP crystal; (*8*) YAG : Nd laser; (*9*) television camera; (*10*) infrared read radiation; (*11*) infrared and second-harmonic write radiations.

The beams were focused in the interior of a 3-mm sample of ZhS18 glass by lenses with a focal length of 3 cm. The generated signal was recorded by a television system and a sampling voltmeter, linked to a computer. Spatial filtering of the photoinduced second-harmonic signal generated by the induced grating made it possible to identify reliably the useful signal against the background associated with the back-reflected second-harmonic write radiation. The signal-to-background ratio was ~ 10/1. Special measures were taken to ensure spatial stability of the photoinduced second-harmonic radiation during these experiments.

The experiments consisted of two stages: the formation (recording) stage beginning with opening of a shutter (*5*) in front of an objective, and the stage of erasing the induced nonlinearity by the read radiation, which began when the

write radiation outside the signal arm was interrupted by a shutter (*6* in Fig. 1). The operating time of the shutters was ~ 0.2 s and the time resolution of the recording system was 0.3–0.5 s (the latter was determined by the television camera used).

The experimental dependence of the signal representing the photoinduced second harmonic and obtained for coincident pulses is plotted in Fig. 2. The initial part (0–30 s) corresponded to the back-scattering of the initial second harmonic by the first shutter (*5*). When this shutter (*5*) was opened at $t \sim 30$ s, the second-harmonic signal rose rapidly and this was followed by a slower rise. Closing the second shutter (*6*) at $t \sim 220$ s induced very fast relaxation of the photoinduced second-harmonic signal, which changed to slow relaxation. The residual second-harmonic signal was approximately equal to the signal growing because of the slow component. The fast component was observed only when the read and write pulses coincided. The efficiency of the photoinduced SHG reached $\sim 5 \times 10^{-9}$, which corresponded to a quadratic nonlinearity of $\sim 1.5 \times 10^{-16}$ m V^{-1}. If the crystallite concentration was assumed to be $\sim 3 \times 10^{-3}$, the photoinduced quadratic nonlinearity in a crystallite amounted to $\sim 5 \times 10^{-14}$ m V^{-1}.

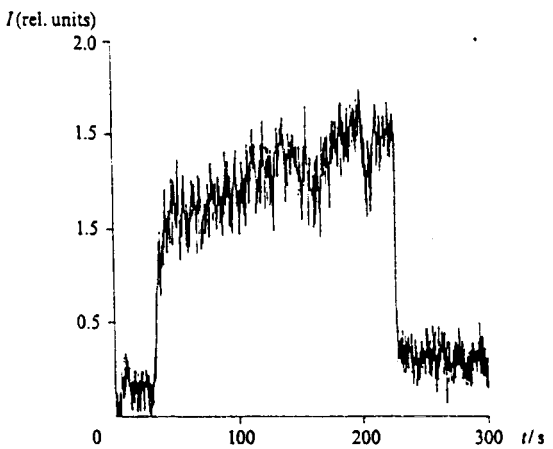

Figure 2. Time dependence of the photoinduced second-harmonic signal *I*. The time $t \approx 30$ s corresponded to the beginning and $t \approx 230$ s to the end of the recording of the photoinduced second harmonic.

Fig. 3 shows in greater detail the fast rise and fast relaxation of the photoinduced second-harmonic signal, which we attributed to a transient nonlinear hologram (grating) of the quadratic susceptibility in the investigated GDSM, induced because of the coherent photogalvanic effect. To the best of our knowledge, such nonlinear holograms have not been observed before.

6. Discussión of results

When the read process proceeded during the write pulse we found that the photoinduced second-harmonic signal increased continuously throughout the write time. This experiment confirmed the predominant contribution of the photogalvanic effect to the photoinduced SHG in a GDSM. We concluded that the fast component of the rise and relaxation of the second harmonic is associated with free carriers in crystallites and with shallow traps, whereas the slow

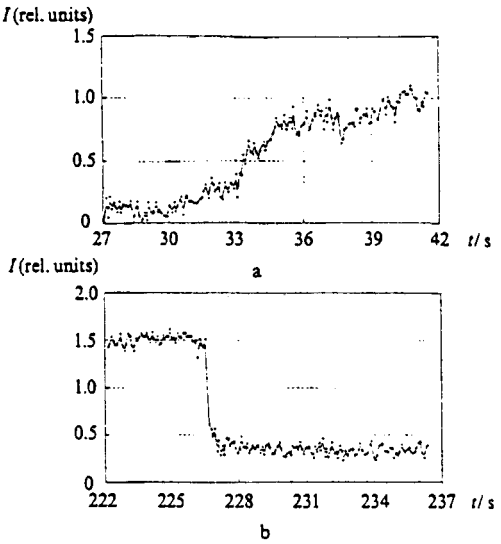

Figure 3. Time dependences of the fast component of the rise (a) and relaxation (b) of the photoinduced second-harmonic signal. The time resolution of the recording system (0.3–0.5 s) was governed by the photographic camera used. The time $t \approx 30$ s corresponded to the beginning and $t \approx 227$ s to the end of the recording of the photoinduced second harmonic.

component is due to the capture of these carriers by deep traps which are probably also present in a glass.

The rise of the signal can be described by the photogalvanic mechanism. If the current density is $\sim 10^{-7}$ A cm^{-2} and the crystallite size is $d \sim 30$ nm, the charge q and the corresponding field $\mathscr{E}_{dc} \sim q/d^2\varepsilon_r\varepsilon_0 \sim 3 \times 10^4$ V cm^{-1} may appear in a time of the order of 1 s (if the relaxation processes are ignored). The relative permittivity of CdS is $\varepsilon_r \sim 8.9$.

The equilibrium charge density in semiconductor microcrystallites is $\sim 10^{-15}$ cm^{-3} [15] and the corresponding relaxation times of the space charge are in the picosecond range. Simple estimates indicate that two-photon absorption of the read wave increases the carrier density by a further several orders of magnitude, so that the instantaneous relaxation of the fast component of the nonlinearity (associated most probably with the release of carriers from relatively shallow traps) is readily understood. It is interesting to note the similarity of the dynamic nonlinearity to transient holograms in semiconductors [16].

It seems strange that we did not observe the contribution associated with the optical rectification effect. One possible explanation of this result is as follows. For the intensities used in our experiments ($E_\omega^2 \approx 8 \times 10^{15}$ V^2 m^{-2} and $E_{2\omega} \approx 6 \times 10^6$ V m^{-1}), even in the case of a resonant cubic nonlinearity ($\sim 10^{-17}$ m^2 V^{-2}), the optical rectification field does not exceed 250 V cm^{-1}. Since $\chi^{(3)}$ of a GDSM is proportional to the linear absorption [17], we may conclude that excitation at the wavelength of 532 nm is nonresonant for ZhS18 glass. In fact, the absorption at the wavelength 532 nm is ~ 0.1 cm^{-1}, i.e. it is approximately two orders of magnitude less than the resonant value. If we assume that the cubic nonlinearity is nonresonant ($\chi^{(3)} < 10^{-19}$ m^2 V^{-2}), the optical rectification field in a microcrystallite can be estimated. This estimate gives no more than 2.5 V cm^{-1}, whereas an experimentally observable

quadratic nonlinearity would require a field in excess of 10^3 V cm^{-1}. The results of our experiments do not, however, negate the possibility of the optical rectification mechanism, which may occur in the resonant case when high intensities are employed.

7. Conclusions

The proposed and implemented experimental method makes it possible to separate the contributions of the optical rectification and coherent photogalvanic effects to the photoinduced SHG. The method is based on a significant difference between the dynamics of the photoinduced nonlinearity at the moment of action of a write pulse in the case of these two processes. The results of experiments carried out by the proposed method support the photogalvanic mechanism of the photoinduced SHG in glasses doped with semiconductor microcrystallites. A fast component of the photoinduced second harmonic observed in these experiments is attributed to transient holograms (gratings) of the quadratic susceptibility.

We are grateful to D Yu Stepanov for his help in this investigation. One of us (D S Starodubov) is indebted to the Moscow Physics Society for the Young Scientist Prize.

References

1. Osterberg U, Margulis W *Opt. Lett.* **11** 516 (1986)
2. Dianov E M, Kazansky P G, Starodubov D S, Stepanov D Yu *Sov. Lightwave Commun.* **2** 83 (1992)
3. Dianov E M, Kazansky E M, Prokhorov A M, Starodubov D S, Stepanov D Yu *Sov. Lightwave Commun.* **2** 147 (1992)
4. Baskin E M, Éntin M V *Pis'ma Zh. Eksp. Teor. Fiz.* **48** 554 (1988) [*JETP Lett.* **48** 601 (1988)]
5. Dianov E M, Kazanskiĭ P G, Stepanov D Yu *Kvantovaya Elektron. (Moscow)* **16** 887 (1989) [*Sov. J. Quantum Electron.* **19** 575 (1989)]
6. Entin M V *Fiz. Tekh. Poluprovodn.* **23** 1066 (1989) [*Sov. Phys. Semicond.* **23** 664 (1989)]
7. Dianov E M, Kazanskiĭ P G, Stepanov D Yu *Kvantovaya Elektron. (Moscow)* **17** 926 (1990) [*Sov. J. Quantum Electron.* **20** 849 (1990)]
8. Baranova N V, Zel'dovich B Ya, Chudinov A N, Shul'ginov A A *Zh. Eksp. Teor. Fiz.* **98** 1857 (1990) [*Sov. Phys. JETP* **71** 1043 (1990)]
9. Anderson D Z, Mizrahi V, Sipe J E *Opt. Lett.* **16** 796 (1991)
10. Dianov E M, Kazansky P G, Starodubov D S, Stepanov D Yu *Proc. SPIE Int. Soc. Opt. Eng.* **2044** 11 (1993)
11. Lawandy N M, MacDonald R L *J. Opt. Soc. Am. B* **8** 1307 (1991)
12. Stolen R H, Tom H W K *Opt. Lett.* **12** 585 (1987)
13. Ouellette F, Hill K O, Johnson D C *Opt. Lett.* **13** 515 (1988)
14. Dianov E M, Kazanskiĭ P G, Starodubov D S, Stepanov D Yu *Trudy IV Mekhdunar. Konf.* '*Problemy Svyazi i Obrabotki Informatsii*', *Sevastopol, 1993* (Proceedings of Fourth International Conference on Communication and Data Processing Problems, Sevastopol, 1993) p. 12
15. DeLong K W, Gabel A, Seaton C T, Stegeman G I *J. Opt. Soc. Am. B* **6** 1306 (1989)
16. Eichler H J, Hartig C, Knof J *Phys. Status Solidi A* **45** 433 (1978)
17. Roussignol P, Richard D, Lukasik J, Flytzanis C *J. Opt. Soc. Am B* **4** 5 (1987)